PERGAMON

International Journal of Heat and Mass Transfer 45 (2002) 367–379

International Journal of HEAT and MASS TRANSFER

www.elsevier.com/locate/ijhmt

An investigation of microscale explosive vaporization of water on an ultrathin Pt wire

S. Glod [a], D. Poulikakos [a,*], Z. Zhao [a], G. Yadigaroglu [b]

[a] *Laboratory of Thermodynamics in Emerging Technologies, Swiss Federal Institute of Technology, ETH Zentrum Institute of Engergy Technology, CH-8092 Zurich, Switzerland*

[b] *Nuclear Engineering Laboratory, Swiss Federal Institute of Technology, Institute of Energy Technology, CH-8092 Zurich, Switzerland*

Received 25 January 2001; received in revised form 30 March 2001

Abstract

The explosive vaporization of water close to its superheat limit was investigated at the microscale level using a short (1 mm in length) and ultrathin (10 μm in diameter) Pt wire. It was possible to obtain novel visualizations and simultaneously pressure and temperature measurements in the vapor microregion, thus accomplishing a step forward in understanding the complex behavior of explosive vapor nucleation, growth, and subsequent collapse, despite experimental difficulties posed by the very short time and length scales of the phenomena. The temperature results verify (to the best of our knowledge, for the first time) the limit of superheat reported in the classical work of Skripov. The nucleation temperature increases with heating rate until a maximum limit is reached. The maximum heating rate was 86×10^6 K/s and a maximum nucleation temperature of 303°C could be obtained. For the visualization of the very rapid boiling process, a strobe microscopy technique was developed and employed. A clear difference in the mode (homogeneous vs. heterogeneous) of vapor nucleation between high and moderate heating rates was observed. A fast pressure transducer allowed to capture the acoustic emission from the expanding vapor volume. From these data, the pressure inside the growing vapor layer and the mechanical energy released by its rapid expansion could be estimated. © 2001 Published by Elsevier Science Ltd.

Keywords: Bubble growth; Microscale; Non-equilibrium

1. Introduction

When a liquid is superheated above its boiling point to temperatures near or at the homogeneous nucleation limit, an abrupt phase change occurs which results in explosive vaporization. Microscopic vapor explosions have been generated by heating liquids rapidly with thin-film microheaters [1–4], thin wires [5–8] and high energy laser beams [9,10].

The kinetic energy from rapidly expanding microbubbles can, in principle, be utilized to drive micromechanical systems. A case in point is the commercial success of thermal ink-jet (TIJ) printers, where the ink is heated rapidly on microheaters and tiny ink droplets are propelled through an orifice by the growth of exploding microbubbles [11]. Successful extraction of the work from the high pressure pulses generated by the microscopic vapor explosions could revolutionize the design and application of thermal micromachines.

Despite current commercial success of the TIJ technology (developed partially by trial-and-error), our knowledge of the *explosive vaporization process* at the microscopic level on a heated surface is limited. Indeed, the fluid dynamics and thermodynamics of microscopic vapor explosion are very complicated during both the initiation and propagation stages. Inconsistent findings and conclusions have been reported in the literature for the mechanism of initiation of microscopic vapor

* Corresponding author. Tel.: +41-1-632-2738; fax: +41-1-632-1176.

E-mail address: poulikakos@ltnt.iet.mavt.ethz.ch (D. Poulikakos).

0017-9310/02/$ - see front matter © 2001 Published by Elsevier Science Ltd.
PII: S0017-9310(01)00158-2

Nomenclature

k	Boltzmann constant (1.3805×10^{-23} J/K)
m	mass of one molecule of the liquid
N	number of liquid molecules per unit volume
p_l	acoustic pressure in the liquid
p_o	ambient liquid pressure
p_v	vapor pressure within the bubble
P_{el}	electric power input
$P_{el,I}$	electric power input at point of boiling incipience
P_m	mechanical power
$P_{m,max}$	maximum mechanical power
Q	thermal energy produced in the Pt wire
Q_l	total thermal energy produced in the Pt wire until boiling incipience
r	distance from Pt wire sample to sensor
R	bubble radius
R_{2-4}, R_s, R_p	constant resistances in bridge circuit setup
R_5	variable resistance in bridge circuit setup
R_W	resistance of Pt wire
R_{W0}	Pt wire resistance at room temperature
t	time
T	Pt wire temperature
T_l	liquid temperature
t_p	duration of voltage pulse
T_{sh}	superheated liquid temperature at boiling incipience
V	volume
V_e	electric pulse voltage
V_{in}	voltage input to the Wheatstone bridge
V_o	voltage input from pulse generator
V_{out}	voltage change across the middle of the bridge
V_W	voltage over Pt wire sample
M	molecular weight
W	mechanical work

Greek symbols

μ_l	liquid viscosity
ρ_l	liquid density
ρ_W	resistivity of Pt wire
σ	liquid surface tension
θ	contact angle
//	product of resistances in parallel

explosion [1,11–15]. Inconsistency also exists among experimental measurements of the maximum fluid temperatures reached before explosive vaporization on microheaters. Existing theories and models do not predict the development of the thermodynamic parameters, such as temperature and pressure, during microscopic vapor explosion.

In a previous work [2] we investigated the explosive boiling process on thin-film microheaters. The boiling process was visualized, quantitative measurements of the pressure transients generated from an exploding microbubble were provided and it was attempted to quantify the amount of mechanical work released into the surrounding liquid from this phenomenon. Temperature measurements were outside the scope of that work. A recent study [16] provides a method for measuring the average surface temperature of a small thin-film microheater. On the other hand, large temperature gradients may exist on the heater surface. In the present study we investigate the explosive boiling process of pure water on an ultrathin practically isothermal Pt wire and provide simultaneously novel visualization results and simultaneous temperature and pressure measurements in the vapor microregion.

2. Experiment

According to Skripov [17], the heating rate of the liquid has to be high-enough for explosive boiling to occur on a heat-releasing surface. To obtain a high heating rate, the thermal mass of the heater should be as small as possible. In the so-called pulse heating experiments, the liquid is in contact with a thin wire or a film microheater that is subjected to a very short and intense electrical pulse. During a very short time period a very large amount of energy is transferred to the liquid. The wire or heater temperature increases rapidly (at a rate higher than 10^7 K/s) and after a few microseconds the liquid in contact with the source boils explosively. The typical length for the heating pulse in the TIJ process is around 5 μs. It is clear that with such short heating pulses, a precise temperature measurement is very difficult because commercially available temperature sensors are not able to respond to such short transients.

A promising method for measuring the temperature of the liquid is based on the measurement of the change of the resistance of the heater or wire during application of the electrical pulse. Careful calibration of the source yields a temperature resistivity coefficient and thus enables us to determine its temperature, as long as an electrical current is applied to the system. For the very small Biot number in the present cases of very thin microheaters or wires, there will be no significant temperature gradients inside the wire. The fluid at the liquid/solid interface can be assumed to be at the average wire temperature. The nucleation incipience temperature can be identified from the change of slope of the temperature curve when the fluid in contact with the wire changes

phase, because when the vapor phase covers the wire, it reduces the rate of heat transfer to the fluid. Fig. 1 shows the typical shape of the temperature curve during application of a heating pulse to a Pt wire in contact with a liquid. The inflection point clearly identifies the moment where explosive boiling is initiated.

In a previous study [2] the pressure pulse emitted from an exploding microbubble on a thin-film microheater was measured. We attempted to use the same microheaters from a commercial TIJ printhead to conduct temperature experiments. In a preliminary study, the temperature distribution on the microheater was investigated with the use of a scanning thermal microscope at steady conditions [18]. For this purpose the microheater was heated up to an equilibrium constant temperature by imposing a low current to the heater. The scanning thermal microscope uses a thermal probe to scan the heater surface and determine its temperature distribution. The experiments showed that the temperature gradients on the heater surface for steady conditions at different input currents, were quite large. Indeed, already at a low average surface temperature of 40°C, temperature gradients of more than 10°C were obtained between the temperature at the center and the temperature at the edges of the microheater.

Based upon these results we decided to use very thin (10 μm diameter) Pt wires (Sigmund Cohn, Mt. Vernon, NY) to carry out the temperature experiments. Platinum is very well suited for this kind of experiments because it has a low conductivity and thus heats up very quickly at relatively low currents compared to other precious metals like gold or silver. In addition, Platinum does not oxidize during the boiling experiments with water and is very robust; this should prevent the wire from breaking when exposed to high thermal stress and cavitation-like effects during the collapse of the vapor film. Compared to the square microheaters with a flat surface of 100×100 μm (for example), the Pt wires used are longer (1 mm) and it can be assumed that thermal losses at the edges of the wire are small compared to the thermal losses at the edges and at the rear of a microheater. Numerical calculations actually show that assuming that the edges of the short wire are maintained at room temperature and the wire is heated to temperatures above 300°C in 5 μs, the difference between the average and the maximum wire temperature due to thermal non-uniformity should indeed not exceed 3%. In a recent numerical study [19] the radial distribution of the temperature was computed for a transient case, taking into account the linear dependence of the electrical resistivity on temperature. It was shown that the radial temperature distribution in the wire heated by a dc electrical current can be assumed uniform.

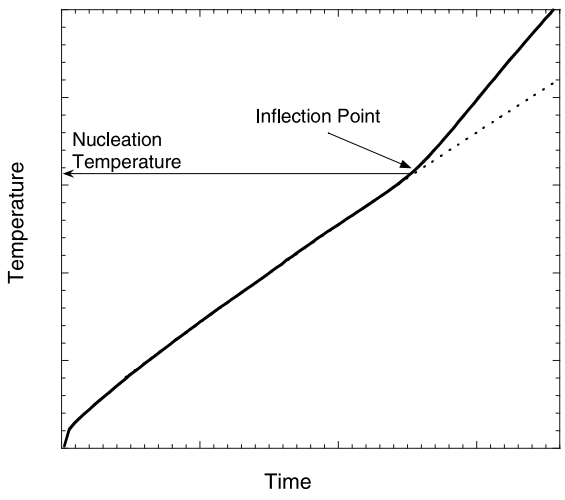

Fig. 1. Typical wire temperature change during application of a heating pulse.

2.1. Experimental setup

The setup used for pressure measurement and visualization is similar to the setup used in a previous study [2]. Pt wire samples were soldered to two stiff, gold-plated connectors (Fig. 2) solidly fixed on a glass substrate. A special, elastic glue was used to better hold the wire and stretch it over the gold connectors. A very thin soldering iron, together with soldering paste, were then used to tightly fix the Pt wire to the stiff connectors. The edges of the connectors were designed in order to plug in the cables supplying the current pulse to the setup. The acoustic pressure wave emitted from the microheater surface was measured by a pressure transducer (Kistler high-frequency quartz pressure sensor 603 B, Kistler Instrumente AG, Winterthur, Switzerland) mounted on a precision slide and facing the surface of the Pt wire. The pressure transducer used in the present study had a natural frequency of 400 kHz. This model of pressure transducer was reported to be able to record the acoustic pressure waves produced from the explosive boiling of a butane droplet at its superheat limit temperature by different groups [20,21]. The pressure transducer generates an electrostatic charge signal corresponding to the received pressure signal. This signal is transformed into a voltage signal, amplified by the charge amplifier (Type

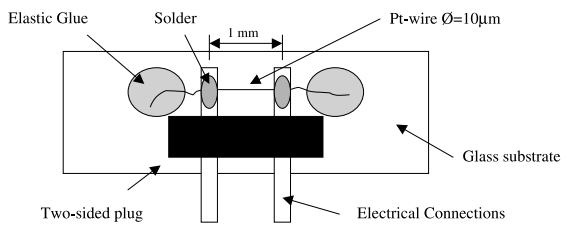

Fig. 2. Topview of the Pt wire heater.

5007 Charge Amplifier, Kistler Instrumente AG, Winterthur, Switzerland) and recorded by an oscilloscope (LeCroy LC 334 A) with a resolution of 500 points per μs. The recorded data are transferred from the oscilloscope to a personal computer for analysis. In an experiment, both the Pt wire and the pressure transducer are immersed in a body of subcooled water open to the atmospheric pressure. The dimensions of the container are 300×100 mm and the water is filled in to a height of 80 mm. Simultaneously with the pressure measurement, the wire temperature is monitored using the dynamic bridge setup, described below.

To visualize the explosive vaporization, the Pt wire, immersed into the pool of subcooled, pure, degased water is placed under a microscope (Olympus BX60) with 50 times magnification. A CCD camera (Pulnix TM795) mounted on the microscope records the boiling process. A Xenon flash lamp (Hamamatsu L4634), synchronized with the heating pulse signal, is controlled by a delay unit that allows the CCD camera to capture individual images at various stages of the boiling process. These images can be mapped to the corresponding points on the pressure trace.

2.2. Temperature calibration

A central issue for obtaining meaningful temperature measurements is careful calibration of the ultrathin Pt wire. In the literature, no data could be found for wires with such small diameters. Although the 10 μm diameter Pt wires are very pure, it cannot be presumed that the temperature-resistance coefficient is the same for very thin wires as for thicker wires.

For the calibration Pt wires of lengths between 5 and 30 mm were used. It was shown that the length of the wires did not affect the temperature coefficient of resistance. The resistance of the Pt wire is measured using the four-wire technique described below. The Pt wire is attached to flexible wires in a computer controlled furnace (Thermolyne Furnace 1300) using high-temperature solder. The procedure for calibration consists of gradually raising the furnace temperature, and simultaneously measuring the furnace temperature and the Pt wire resistance using a HP 3852A data acquisition unit. The furnace temperature is measured by taking the average readings of two fine thermocouples (Type K) mounted very close to the Pt wire sample. The temperature difference between the two thermocouples never exceeded 1°C. The furnace temperature was raised in small time steps and held at a constant level after each step until the temperature of the furnace and the resistance of the Pt wire were stabilized.

Fig. 3 shows the resistivity vs. temperature curve obtained for different samples under different heating conditions. It can be seen that the resistivity is a linear function of temperature and that the results obtained are very consistent. Our data agree well with data obtained for thicker wires [22]. No hysteresis effect could be observed. In similar experiments performed with microheaters, a recently published study [16] showed a marked hysteresis effect with temperature that seemed to decrease and practically disappear only after repeated temperature cycling. Another advantage (from the standpoint of accuracy) of using Pt wires instead of microheaters from TIJ printheads is that the resistivity dependence on temperature is an order of magnitude larger for platinum than for the typical material used in microheaters (alloy of Aluminium and Tantalum).

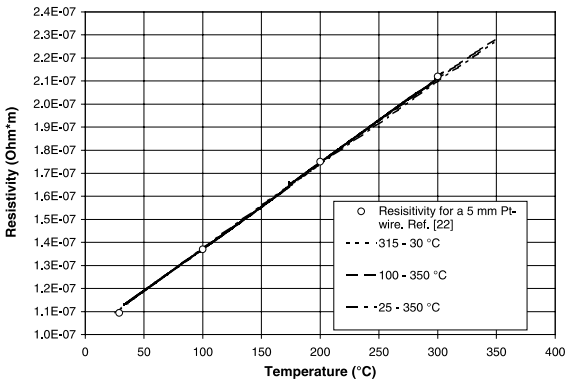

Fig. 3. Calibration curves. Resistivity as a function of temperature for a 10 μm Pt-wire.

The final calibration curve deduced from our experiments is given by:

$$T = 2.72 \times 10^9 \rho_W - 275, \tag{1}$$

where T is the wire temperature in °C and ρ_W the specific resistivity of the wire (Ωm). In practice, the initial resistance of the Pt wire is determined at room temperature, the change in resistance is monitored during the heating process, and the temperature is deduced from the calibration curve.

2.3. Electronic circuit and bridge setup

To determine the temperature of the previously calibrated Pt wires, their resistance is measured during the application of the heating pulse. Fig. 4 shows the electronic circuit designed to apply short and intense current pulses to the Pt wire and to simultaneously measure fine changes in wire resistance. Because of its outstanding sensitivity, the well-known Wheatstone bridge setup for measuring the change in wire resistance is used. To reduce the effect of the impedance of the extension wires on the resistance measurement, a four-wire configuration is used. The four wires are perfectly matched in length so that their impedances cancel because each is in an opposite leg of the bridge. Two wires lead the current

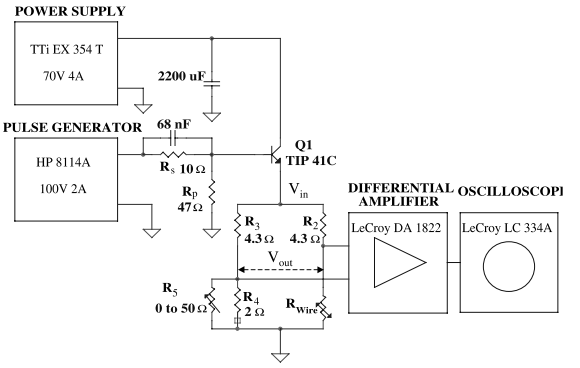

Fig. 4. Schematic of the electronic circuit.

to and from the sample, while the other two carry the measured signal.

In order to be able to apply short, high-current square pulses with very short rise and fall times to the Pt wire, an emitter–follower arrangement had to be designed. Pulse durations of less than 10 μs with currents up to 4 A are required to obtain the desired explosive vaporization. Where the common emitter amplifier requires a voltage-to-current converter input, the emitter–follower configuration requires a voltage input only. The square voltage pulse is provided by a HP 8114A programmable pulse generator that controls pulse duration, t_p and voltage V_0. The necessary current is provided by a power supply (TTi Ex 354).

The initial resistance R_{W0} of the Pt wire is measured using a high precision RCL meter (Philips PM 6303). The voltage signal V_{out} from the bridge, which is a function of input voltage to the bridge, V_{in}, bridge completion resistances and Pt wire resistance, is measured with a differential amplifier. V_{in} and V_W, the voltage across the Pt wire, are also constantly measured and displayed on the oscilloscope.

The wire resistance R_W is continuously increasing during the application of the heating pulse and can be calculated from the following equation:

$$R_W = \frac{R_2\left(\frac{V_{out}}{V_{in}} + \frac{R_{W0}}{R_2+R_{W0}}\right)}{1-\left(\frac{V_{out}}{V_{in}} + \frac{R_{W0}}{R_2+R_{W0}}\right)}, \tag{2}$$

where R_{W0} is the initial resistance of the Pt wire and R_2 $(= R_3)$ the resistance in the upper leg of the bridge.

The thermal energy, Q, produced in the ultrathin Pt wire can be calculated from

$$Q = \int_0^{t_p} \frac{V_W^2}{R_W}\,\mathrm{d}t. \tag{3}$$

For analysis of the results it is also important to calculate the instantaneous electric power input, P_{el}, to the Pt wire,

$$P_{el} = \frac{V_W^2}{R_W} \tag{4}$$

and record the temperature gradient during the application of electric power. During the application of the heating pulse, the power input to the Pt wire is not constant due to the change in wire resistance. The increase of input power from the beginning of the pulse until the point of boiling incipience is of the order of 60%. For the data analysis, the power input at the point of nucleation incipience, $P_{el,I}$ will be employed to compare the results for different power inputs and heating rates.

3. Results

Fig. 5 shows the progressive stages of explosive vaporization of water on the thin Pt wire. A Xenon flash lamp, synchronized with the heating pulse signal, is controlled by a delay unit that allows a CCD camera to capture individual bubble images at various stages of the boiling process. In this example the length of the applied current pulse is 8 μs, the applied electrical power equals 24 W (≈ 800 MW/m^2), the adiabatic wire heating rate is 50×10^6 K/s and the total energy input Q_i until the start of explosive boiling is 120 μJ. In the following, these conditions are referred to as the "reference case". It can be seen that approximately 7 μs after the beginning of the heating pulse, the water begins to boil explosively along the entire length of the Pt wire. The initially coherent vapor film (difficult to see in the scale of Fig. 7 but an enlarged version of this region will be shown below) breaks up into separate subregions that continue to grow, even after the heating pulse has terminated. When these microbubbles (vapor regions) finally seem to have disappeared, they reappear, *in the absence of external heating* (the electrical pulse lasts only 8 μs as mentioned earlier), and approximately 17 μs after the initiation of the pulse. This reappearance or regrowth of the vapor bubbles is comparable to similar observations made during the explosive boiling of water on flat thin-film microheaters [2].

In the present paper we focus on the simultaneous measurement of the acoustic pressure wave emitted by the exploding vapor layer and the superheat temperature of the liquid at boiling occurrence. It is well known that when a bubble in a liquid undergoes expansion or contraction, acoustic pressure waves are radiated from the bubble surface [23]. This pressure is called acoustic pressure. The pressure produced within the vapor micro layer during microscopic vapor explosion provides the "driving force" for the motion of the bulk liquid. The pressure transient propagates from the vapor region into the surrounding liquid by the interface between vapor and liquid. The intensity of the acoustic pressure waves

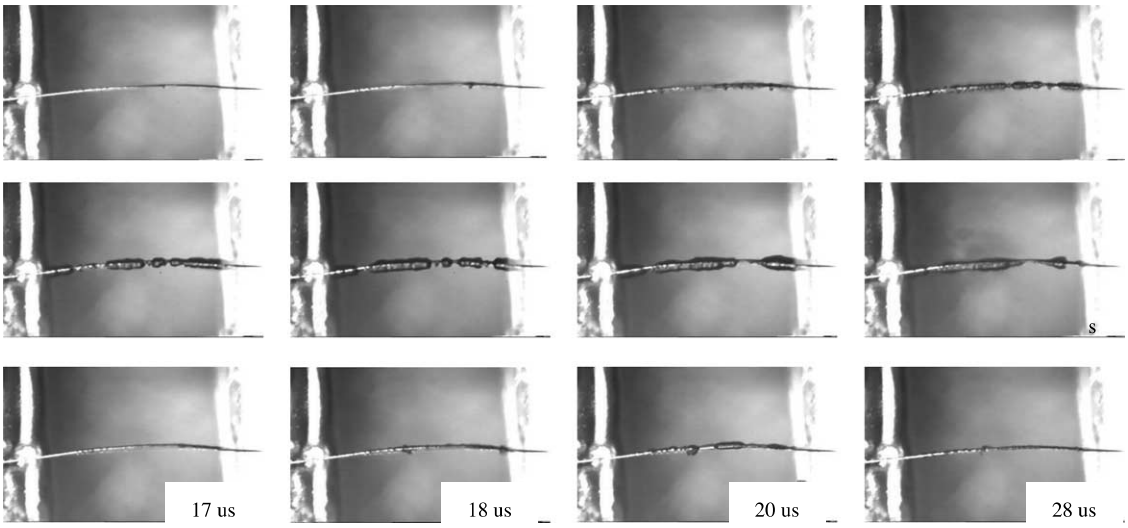

Fig. 5. Progressive stages of explosive vaporization of water on an ultrathin Pt-wire for a 24 W, 8 μs heating pulse.

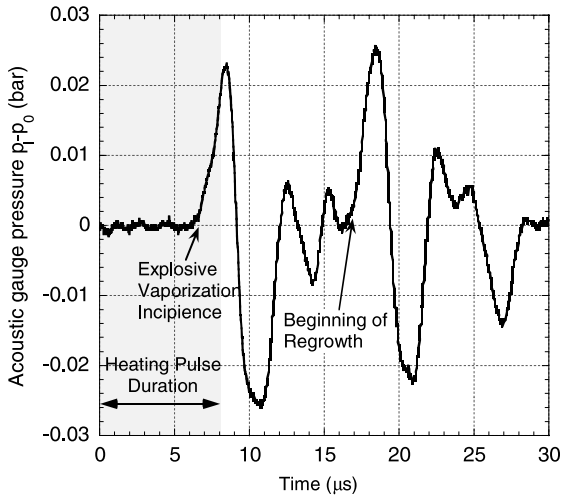

Fig. 6. Acoustic waveform for a 24 W, 8 μs heating pulse.

represents the intensity of the microscopic vapor explosion on the Pt wire surface, which again is a function of the superheat of the liquid before explosive vaporization occurs. Fig. 6 shows a typical pressure wave produced by the explosive boiling of water on the Pt wire measured at transducer-to-microheater distance $r = 20$ mm for the reference case ($t_p = 8$ μs, $P_{el,I} = 24$ W). The acoustic pressure is characterized by two large positive pressure pulses, each immediately followed by a negative pressure pulse. A similar pressure trace was obtained for the dynamic growth of a vapor bubble on thin-film microheaters [2,23,24]. The first positive pressure pulse corresponds to the generation and expansion of a vapor microlayer on the microheater, which launches a compression wave into the surrounding liquid. The second positive pressure pulse is generated after the implosion of the contracting vapor layer and is the result of regrowth (rebounding) of the vapor bubble. The positive and negative values of the acoustic pressure wave correspond to the acceleration ($d^2V/dt^2 > 0$) and deceleration ($d^2V/dt^2 < 0$), respectively, of the vapor volume growth.

The pressure transducer is located at a distance of 20 mm from the Pt wire and has a diameter of 4 mm and the Pt wire sample has a length of 1 mm. This allows us, when viewed from the transducer, to consider the exploding vapor layer as a spherical oscillating gas volume. The assumption of a spherical vapor volume does not fully correspond to the Pt wire experiment, but nevertheless allows us to estimate the pressure inside the growing vapor layer and the mechanical energy released from its rapid expansion. Under these idealized conditions, the acoustic pressure wave in the liquid, p_l, emitted by the growing spherical vapor volume can be calculated by integrating the transient Euler equation in the radial direction to a point in the liquid at a distance r from the bubble center:

$$p_l(r,t) - p_o = \frac{\rho_l R}{r}\left[2\left(\frac{dR}{dt}\right)^2 + R\frac{d^2R}{dt^2} - \frac{1}{2}\left(\frac{dR}{dt}\right)^2\left(\frac{R}{r}\right)^4\right], \tag{5}$$

where p_o is the ambient liquid pressure surrounding the source, t the time, R the bubble radius and ρ_l the liquid density. Using the measured acoustic pressure on the left-hand side of this equation, the radius of the bubble can be obtained. In the present experimental setup, with $r \gg R$, the third term in Eq. (5) is negligible.

Applying the Laplace equation at the vapor/liquid interface ($r = R$),

$$p_v = p_l + \frac{2\sigma}{R} \tag{6}$$

the classical Rayleigh–Plesset equation is obtained from Eq. (5) and the vapor pressure within the bubble, p_v, can be calculated.

$$p_v(t) - p_o = \rho_l R \frac{d^2R}{dt^2} + \frac{3}{2}\rho_l \left(\frac{dR}{dt}\right)^2 + \frac{2\sigma}{R}, \tag{7}$$

where σ the liquid surface tension. The liquid viscosity can be assumed to have a negligible effect in these experiments.

As mentioned before, the kinetic energy transferred from the expanding vapor into the surrounding liquid can be used, in principle, to drive electromechanical microdevices such as micro actuators and pumps. Information about the useful work that can be obtained from the thermal energy on the surface of a microheater is important for these applications. Part of the mechanical work is used to overcome the ambient pressure and to increasing the vapor/liquid interface surface area. Hence, it is not available as useful energy. The useful extractable mechanical work, $W(t)$, can then be calculated by,

$$W(t) = \int_0^t \left[p_v - p_o - \sigma\left(\frac{32\pi}{3V(t)}\right)^{1/3}\right] \frac{dV(t)}{dt}\, dt \tag{8}$$

assuming that the vapor layer surface area can be approximated by the surface area of a spherical bubble with the same volume.

The corresponding mechanical power, P_m, is the integrand in the above integration,

$$P_m = \frac{dW(t)}{dt}. \tag{9}$$

Fig. 7 shows the bubble excess pressure, $p_v - p_o$, calculated from Eq. (7) and the extractable mechanical power calculated from Eq. (9), under the spherical bubble assumption for the reference case ($t_p = 8$ μs, $P_{el,I} = 24$ W).

In the present study pressure experiments have been performed for different voltage pulses. For higher input voltage the pulse length had to be reduced in order to prevent burn out of the wire. In Table 1 the average results for different experiments are summarized. Eq. (4) gives the input power at the inflection point, $P_{el,I} \cdot Q_I$, the total energy input until the initiation of explosive boiling can be calculated from Eq. (3). The heating rate, dT/dt, was deduced from the time vs. temperature plots. The bubble excess pressure, $p_v - p_o$, was calculated from Eq. (7) and the maximum extractable mechanical power, $P_{m,max,}$ was calculated from Eq. (9) (Fig. 7). T_{sh} is the superheat temperature at the point of explosive boiling incipience deduced from the temperature experiments. The displayed data are averaged over at least 10 distinct data sets for every heating case.

From the data obtained for the bubble excess pressure and the extractable mechanical energy, it can be seen that substantially higher mechanical power can be extracted at higher input power. However there seems to be an upper limit to the extractable mechanical power. It can also be seen that there is an upper limit of superheat temperature which could not be exceeded by applying more intense electric pulses to the Pt wire. These results will be discussed in detail later in this paper.

The temperature measurements were performed simultaneously with the pressure measurements as

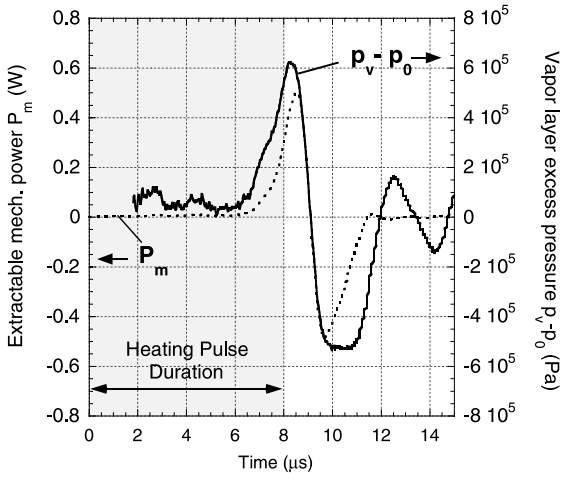

Fig. 7. Extractable mechanical power and vapor layer excess pressure for a 24 W, 8 μs heating pulse.

Table 1
Experimental data gathered for different heating pulses

$P_{el,I}$ (W)	t_p (μs)	Q_I (μJ)	dT/dt (10^6 K/s)	$p_v - p_o$ (bar)	$P_{m,max}$ (W)	T_{sh} (°C)
42.5	4.5	151.5	86	10	0.48	302
35	6	144	74	8.2	0.50	302
32.5	6	144	66	8.1	0.52	303
30	6	144	62	8.0	0.50	302
24	8	140	50	6.2	0.50	293
21	8	136	44	6	0.48	287
7	30	157	10	1	0.08	275

already noted. From the change in Pt wire resistance during the application of the heating pulse, the Pt wire surface temperature was determined. Fig. 8 shows samples of temperature response curves for heating pulses at different power inputs. The time scale on the x-axis represents the length of the heating pulse and it can be seen that the liquid heating rate increases with higher power input. The highest heating rate that was achieved in the present experiments was 86×10^6 K/s.

An accurate measurement of the maximum liquid temperature at the initiation of explosive boiling requires an exact determination of the inflection point on

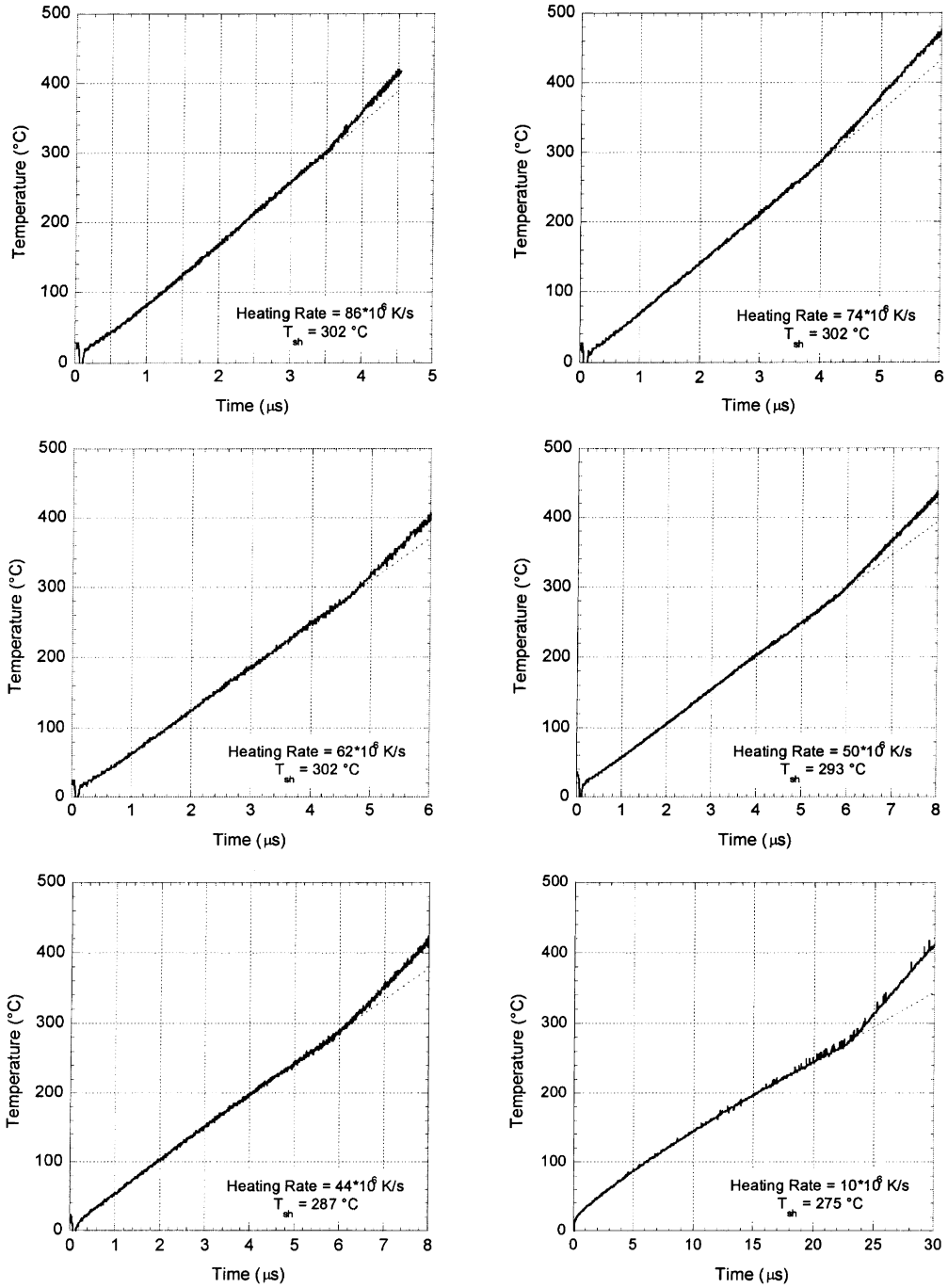

Fig. 8. Temperature response curve of Pt-wire for different heating pulse lengths and input power.

the temperature curve. To this end, the data points situated far enough before the inflection point were curve fitted with a polynomial of third order. This curve fit can also be seen on Fig. 8. The curve fit follows to the shape of the temperature curve up to the point where the temperature trace abruptly changes slope. The point where the data points ceased to follow the curve fit was then determined analytically as the inflection point.

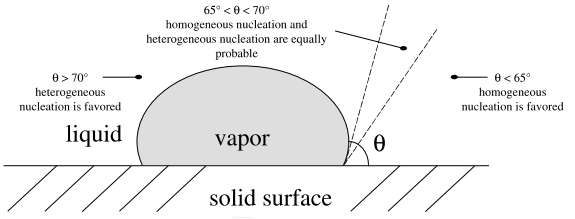

Fig. 10. Embryo bubble formed at an idealized liquid–solid interface.

4. Analysis

4.1. Boiling mechanism and liquid superheat

Fig. 9 shows the variation of nucleation temperature with liquid heating rate. It appears that there exists a limiting heating rate beyond which the attainable superheat temperature is independent of the heating rate. The nucleation temperature increases with input power and approaches a maximum of 303°C, the highest, average, superheat temperature measured in the present study. The data scattering was of the order of ± 4°C for the different heating pulses.

The data can be compared to results calculated in classical nucleation theory for the kinetic limit of superheat. It will be shown that for high heating rates, homogeneous nucleation theory can actually be applied to the present experimental system. Indeed, in the ideal case of a perfectly smooth wire surface, the probability of homogeneous nucleation is always higher than that for heterogeneous nucleation if the contact angle, θ, between the liquid and the solid surface, Fig. 10, is small [25]. For $\theta < 65°$ it was argued that higher superheat is required to initiate heterogeneous nucleation than to obtain homogeneous nucleation [26].This angle range corresponds to the present case of water on Platinum with a theoretical contact angle of 40° [27]. However, the high superheat predicted for the idealized smooth surfaces is rarely observed experimentally because most solid surfaces contain irregularities and boiling is then initiated at temperatures far below the homogeneous limit of superheat by gas trapped in narrow crevices on the solid surface. Only if the heating rates are high enough it is possible to prevent the growing of vapor bubbles from surface imperfections and to heat the liquid around the wire to its limit of superheat.

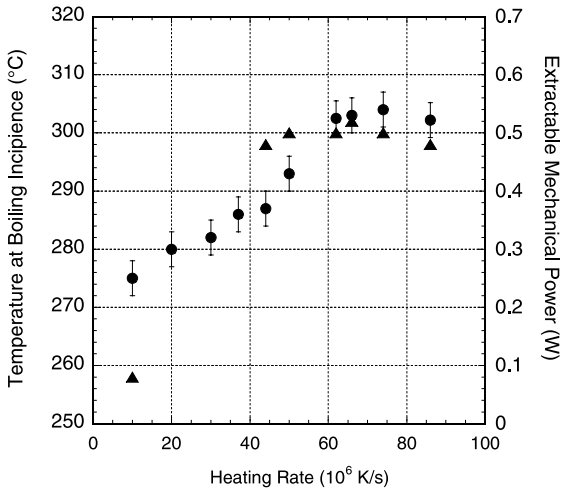

Fig. 9. Superheat temperature of the water at boiling incipience and corresponding extractable mechanical power.

Fig. 9 shows that the heating rate has to be higher than 60×10^6 K/s in order to reach the maximum nucleation temperature, in the present experiment 303°C. This value will be compared to homogeneous nucleation theory results below. For lower heating rates, heterogeneous nucleation seems to be the governing boiling mechanism.

Visualization of the boiling process at different heating rates confirms these observations. Fig. 11 shows the explosive boiling mechanism for the highest heating rate of 86×10^6 K/s. It can be seen that the wire surface is almost instantaneously covered with a thin vapor film. However, images from the initial stages of vaporization seem to show "ready centers" [17] on the wire surface that develop and initiate the explosive boiling process. Homogeneous nucleation seems to occur within a very thin superheated liquid layer which has a very steep temperature gradient and heterogeneous nucleation seems to occur simultaneously on the heating wall [3].

For a low heating rate of 10^5 K/s the nucleation temperature is around 275°C, Fig. 9, and the extractable mechanical work from the growing vapor volume is much lower than for high heating rates. Fig. 12 shows the boiling mechanism for a heating rate of 10^5 K/s and it can be seen that the nucleation is initiated by a single vapor bubble growing from a cavity on the wire surface which then triggers the boiling on the entire wire surface. In this case heterogeneous nucleation is clearly the mechanism that governs the boiling process.

Table 2 shows representative results for the maximum attainable water superheat temperature obtained in previous studies with pulse heating experiments at atmospheric pressure. It can be seen that the results

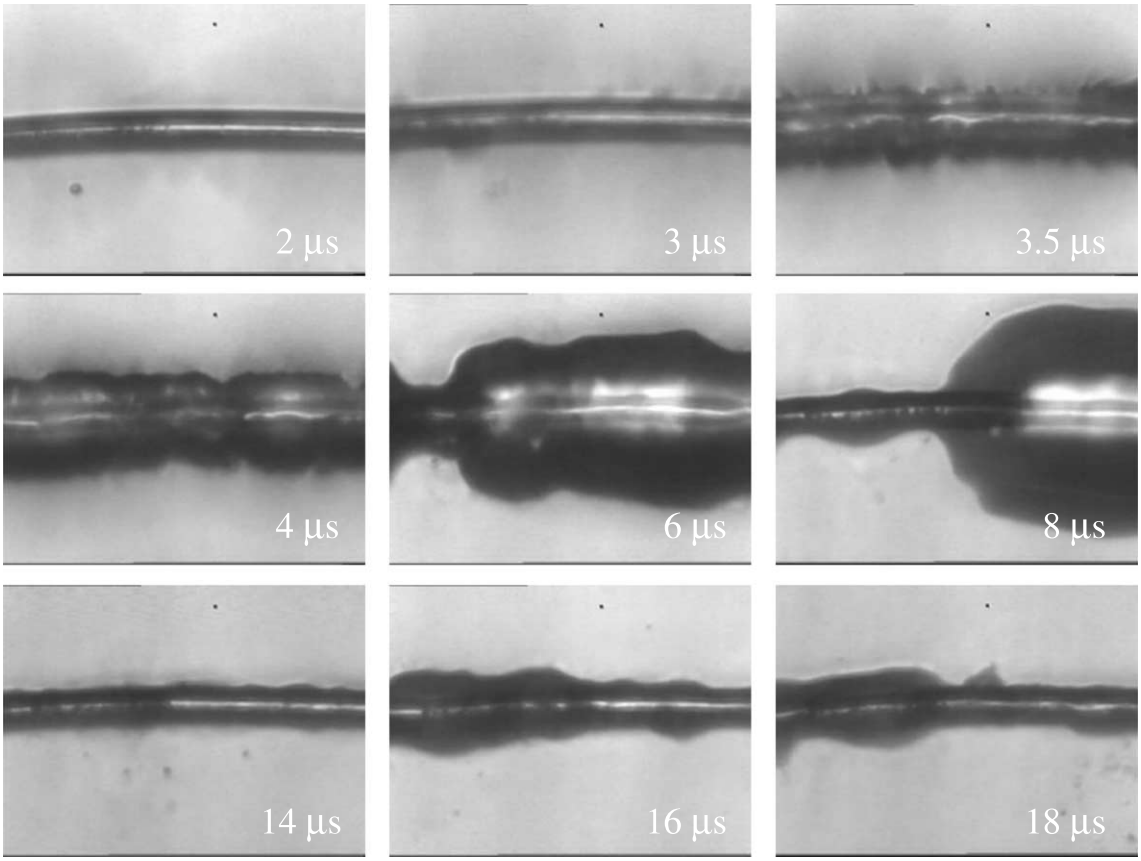

Fig. 11. Progressive stages of explosive vaporization of water on an ultrathin Pt-wire for a 42.5 W, 4.5 μs heating pulse. Heating rate = 86×10^6 K/s.

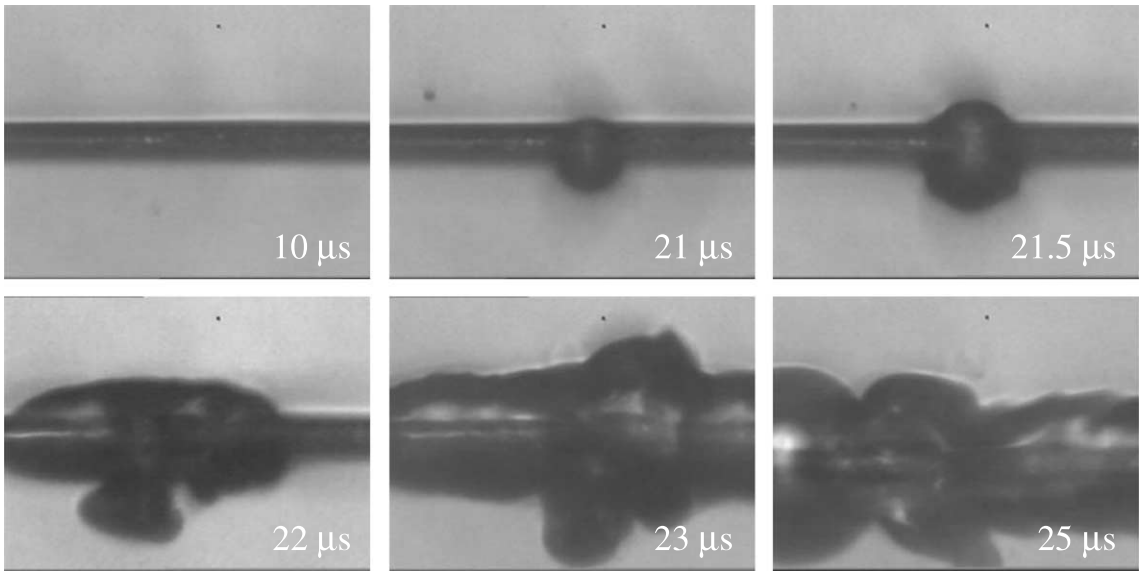

Fig. 12. Initial stages of explosive vaporization of water on an ultrathin Pt-wire for a 7 W, 30 μs heating pulse. Heating rate = 10×10^6 K/s.

Table 2
Measured superheat temperatures for pulse heating experiments at atmospheric pressure

Heating rate (K/s)	Heater	Temperature (°C)	Reference
86×10^6	Pt wire (Ø = 10 μm)	303	Present study
1×10^6	Pt wire (Ø = 20 μm)	302	[5]
93×10^6	Pt film heater	295	[3]
10×10^6	Pt wire (Ø = 25 μm)	290	[8]
250×10^6	Ta–Al film heater	283	[16]

obtained in the present study are at the upper end of the range of previously published data. These results have to be compared to theoretical values obtained for the kinetic limit of superheat.

Vapor nuclei have to be grown above a certain critical size in order to spontaneously grow and initiate homogeneous (or heterogeneous) nucleation. Kinetic theory (with its inherent assumptions) allows to predict the birth rate of such critical size nuclei formed by local fluctuations in a superheated liquid. The theory predicts J, the rate of formation of bubbles which grow beyond a critical size and continue to grow spontaneously [25]. For homogeneous nucleation, J is given by [26]:

$$J = N\sqrt{\frac{3\sigma}{\pi m}}\exp\left(\frac{-16\pi\sigma^3}{3kT(p_v - p_l)^2}\right), \tag{10}$$

where N is the number of liquid molecules per unit volume, m is the mass of one molecule of the fluid and k the Boltzmann constant. Since some of the variables in this equation are dependent on the temperature, the limiting superheat temperature can only be determined by solving it iteratively, having chosen a suitable threshold value for J.

Eq. (10) can be rewritten as [26]:

$$J = 1.44 \times 10^{40}\sqrt{\frac{\rho^2\sigma}{M^3}}\exp\left(\frac{-1.213 \times 10^{24}\sigma^3}{T(p_v - p_l)^2}\right), \tag{11}$$

where M is the molecular weight of the liquid. In practice, from Eq. (11) one calculates J at different temperatures by using saturation-condition values for p_v, σ, ρ_l for water for various T values. Because most of the temperature-dependent quantities in Eq. (11) appear in the exponential term, a slight change in T has a very strong effect on the rate of nucleation. A change of 1°C can change J by as much as three or four orders of magnitude. As the rate of nucleation changes so rapidly with temperature there exists a very narrow temperature range below which homogeneous nucleation does not occur and above which it occurs instantaneously.

For most situations, assuming $J = 10^6$ nuclei/m^3 s will give perfectly acceptable results for the limiting kinetic superheat temperature [28]. With this assumption for J, Eq. (11) yields a limiting superheat temperature T_{sh} of 302°C for water at atmospheric pressure. Van Carey [26] assumes a threshold value for J of 10^{12} nuclei/m^3 s which yields a value of 304°C for the limiting superheat temperature. These values agree very well with experimental data obtained in the present study.

A valid question pertains to the utilization of macroscopic property values for minute quantities of matter (for example the value for the surface tension coefficient of a vapor embryo in Eq. (11)). Although lack of experimental data for properties at the nanoscopic level prevents a better solution, the point should be made that future studies should aim at improving the property database at the lower limits of continuum theory.

One should also not lose sight of the fact that the theory used above and the estimated values are not conclusive and are based on some empiricism and a series of assumptions. Other approaches can lead to different predictions. For example in pulse heating experiments according to another approximate theory (involving also order-of-magnitude arguments), the nucleation rate is expected to be much higher than the value of 10^{12} nuclei/m^3 s used here [29]. A range of achievable nucleation rates (with a pulse heating method) of 10^{21}–10^{28} nuclei/m^3 s was predicted. The reason for this high range of nucleation rates is the large heating rates. In this case, Eq. (11) yields a range 309–314°C for the limiting liquid superheat temperature.

As can be seen from Table 2, for water, pulse heating experimental results for the temperature at boiling incipience are always lower than the predicted homogeneous nucleation temperature range 309–314°C. However, the results agree well with theoretical data at lower range of predicted nucleation temperature.

4.2. Error analysis

The current acoustic pressure transient measurements have uncertainties due to the quartz pressure transducer resonance at its natural frequency and the charge amplifier linearity error. In the pressure range of the present experiment the uncertainty due to linearity error is about 0.2. The error caused by the transducer resonance is less than 5% at 1/3 of its natural frequency and increases with signal frequency. Due to the short heating pulse duration, the dynamic impedance in the

power amplifier and the resistance heating delivery circuits cause uncertainties in the energy input to the microheater. The distance between the pressure transducer and the Pt wire sample is measured by moving the transducer away from the microheater surface after an initial contact between the sample and the transducer where the distance $r = 0$ is assigned. We estimated that the gap between the wire surface and the transducer surface at "contact" can be up to 0.5 mm. In the present case, the relative error is 2.5% of the measured heater-to-sensor-distance of 20 mm. A further source of error is a possible small deviation from the normal angle of incidence between the sample and the transducer. The estimated alignment error is $\pm 2°$. Within this range no variation of the transducer output was detected. The total error of acoustic pressure measurements due to the transducer resonance, the charge amplifier linearity error, and the distance measurement error can be up to 5% of the difference between atmospheric pressure and the measured pressure signal.

Experimental uncertainty in the temperature experiments is partly due to the inaccuracy of the determination of the point where explosive boiling is initiated. One also has to account for errors due to thermal non-uniformity because of possible thermal losses at the edges of the Pt wire. However, a one-dimensional model which we developed estimates the experimental error due to thermal losses at the ends of the wire to 3% of the difference between the wire temperature and room temperature (taken as reference value). Errors due to calibration reproducibility and radial temperature non-uniformity inside the wire are negligible. In the present results, the total error of the temperature measurements is estimated to be within a margin of ± 5°C.

5. Summary

The present study aims at providing a coherent and complete investigation of the behavior of water explosions on a Pt wire at high superheat temperatures. In order to gain a better insight, as well as quantification of the boiling mechanism, visualization, temperature and acoustic pressure measurements were conducted.

The nucleation temperature was determined by measuring the change of resistance of the Pt wire during the application of a heating pulse. The maximum heating rate was 86×10^6 K/s and a maximum nucleation temperature of 303°C could be obtained. The nucleation temperature increases with heating rate until a maximum limit is reached. Visualization of the boiling process shows that at low heating rates and superheat, boiling is clearly initiated by heterogeneous nucleation, whereas, for very high heating rates, boiling approaches the mechanism of homogeneous nucleation. This is confirmed by the fact that the obtained superheat temperatures reach the range predicted by homogeneous nucleation theory.

The dynamics of the vapor phase are reconstructed from the data obtained during acoustic pressure measurements. The maximum value obtained for the pressure inside the vapor layer is estimated to be 10 bar. In order to drive MEMS devices, it is of major importance to be able to estimate the maximum extractable power. An instantaneous peak value of 0.52 W was determined. It is important to notice that at temperatures close to the theoretical superheat limit, the extractable mechanical energy is much higher than at lower temperatures, which means that, in order to reliably drive MEMS devices based on explosive boiling, one has to approach temperatures for the liquid close to its kinetic limit of superheat.

Acknowledgements

The research presented in this paper was supported in part by the Swiss National Science Foundation (contract number: 2100-052327.97/1).

References

[1] A. Asai, S. Hirasawa, I. Endo, Bubble generation mechanism in the bubble jet recording process, J. Imaging Technol. 14 (1988) 120–124.
[2] Z. Zhao, S. Glod, D. Poulikakos, Pressure and power generation during explosive vaporization on a thin-film microheater, Int. J. Heat Mass Transfer 43 (2000) 281–296.
[3] Y. Iida, K. Okuyama, K. Sakurai, Boiling nucleation on a very small film heater subjected to extremely rapid heating, Int. J. Heat Mass Transfer 37 (1994) 2771–2780.
[4] L. Lin, A.P. Pisano, V.P. Carey, Thermal bubble formation on polysilicon micro resistors, ASME J. Heat Transfer 120 (1998) 735–742.
[5] V.P. Skripov, P.A. Pavlov, Explosive boiling of liquids and fluctuation nucleus formation, High. Temp. (USSR 8 (1970) 782–787.
[6] V.P. Skripov, P.A. Pavlov, E.N. Sinitsyn, Heating of liquids to boiling by a pulsating heat supply: 2. Experiments with water, alcohols, *n*-hexane and nonane, High Temp. (USSR 3 (1965) 670–674.
[7] P.A. Pavlov, V.P. Skripov, Boiling of a liquid with pulsed heating: 1. Hot-wire method of experiment, High Temp. (USSR) 3 (1965) 97–101.
[8] K.P. Derewnicki, Experimental studies of heat transfer and vapour formation in fast transient boiling, Int. J. Heat Mass Transfer 28 (11) (1985) 2085–2092.
[9] T. Asshauer, K. Rink, G. Delacrétaz, Acoustic transient generation by holmium laser induced cavitation bubbles, J. Appl. Phys. 76 (1994) 5007–5013.
[10] H.K. Park, D. Kim, C.P. Grigoropoulos, A.C. Tam, Pressure generation and measurement in the rapid vapor-

ization of water on a pulsed-laser-heated surface, J. Appl. Phys. 80 (7) (1996) 4072–4081.
[11] R.R. Allen, J.D. Meyer, W.R. Knight, Thermodynamics and hydrodynamics of thermal ink-jets, Hewlett–Packard J. 5 (1985) 21–27.
[12] W. Runge, Nucleation in thermal ink-jet printers, in: IS & T's Eighth International Congress on Advances in Non-Impact Printing Technologies, 1992, pp. 299–302.
[13] J.R. Maa, C.Y. Tung, The maximum boiling superheat of water, Lett. Heat Mass Transfer 7 (1980) 121–128.
[14] I. Owen, J.M. Jalil, Heterogeneous flashing in water drops, Int. J. Multiphase Flow 17 (5) (1991) 653–660.
[15] S. aus der Wiesche, C. Rembe, E.P. Hofer, Boiling of superheated liquid near the spinodal: I general theory, Heat Mass Transfer 35 (1999) 25–31.
[16] C.T. Avedisian, W.S. Osborne, F.D. McLeod, C.M. Curley, Measuring bubble nucleation temperature on the surface of a rapidly heated thermal ink-jet heater immersed in a pool of water, Proc. R. Soc. Lond. A 455 (1999) 3875–3899.
[17] V.P. Skripov, Metastable Liquids, Wiley, New York, 1974 (Chapters 4 and 6).
[18] R. Zweidler, Kalibration von Messsonden eines Scanning Thermal Microscope und deren Anwendung zur Bestimmung der Temperaturverteilung einer HP Ink Jet Mikroheizung., Semesterarbeit, ETH, Zürich, Switzerland, 1998.
[19] H. Chiriac, I. Astefanoaei, A model of the DC joule heating in amorphous wires, Phys. Stat. Sol. 153 (1996) 183–189.
[20] A. Lesin, H. Baron, H. Branover, J.C. Merchuk, Direct contact boiling at the superheat limit, in: G.F. Hewitt, (Ed.), Proceedings of the 10th International Heat Transfer Conference, Third Edition, 1994, pp. 347–352.
[21] H. McCann, L.J. Clarke, P.A. Masters, An experimental study of vapor growth at the superheat limit temperature, Int. J. Heat Mass Transfer 32 (6) (1989) 1077–1093.
[22] L. Binkele, M. Brunen, Thermal Conductivity, Electrical Resistivity and Lorenz Function Data for Metallic Elements in the Range 273–1500 K, 1994.
[23] J.D. Meyer, Bubble growth and nucleation properties in thermal ink-jet printing technology, SID 86 Digest (1986) 101–104.
[24] M. Sakurai, Kawaharada, M. Tsuzuki, Dynamic analysis of vapor bubble in liquid using acoustic emission measurement, Jap. J. Appl. Phys. 27 (Suppl 27-1) (1988) 79–81.
[25] M. Blander, J.L. Katz, Bubble nucleation in liquids, AIChE J. 21 (5) (1975) 833–847.
[26] V.P. Carey, Liquid–Vapor Phase-Change Phenomena, Hemisphere, London, vol. 112–124, 1992, pp. 138–150.
[27] A.W. Adamson, Physical Chemistry of Surfaces, Wiley, New York, 1990, p. 397.
[28] S.v. Stralen, R. Cole, Boiling Phenomena, vol. 1, Hemisphere, London, 1979.
[29] C.T. Avedisian, The homogeneous nucleation limit of liquids, J. Phys. Chem. Ref. Data 14 (3) (1985) 695–729.